Mon. Not. R. Astron. Soc. **000**, 000–000 (0000) Printed 4 June 2009 (MN LATEX style file v2.2)

Fossil Gas and the Electromagnetic Precursor of Supermassive Binary Black Hole Mergers

Philip Chang[1,2⋆], Linda E. Strubbe[1⋆], Kristen Menou[3⋆], & Eliot Quataert[1⋆]
[1] *Department of Astronomy and Theoretical Astrophysics Center, 601 Campbell Hall, University of California, Berkeley, CA 94720*
[2] *Miller Institute for Basic Research*
[3] *Department of Astronomy, Pupin Hall, Columbia University, 550 West 120th Street, New York, NY 10027*

4 June 2009

ABSTRACT

Using a one-dimensional height integrated model, we calculate the evolution of an unequal mass binary black hole with a coplanar gas disc that contains a gap due to the presence of the secondary black hole. Viscous evolution of the outer circumbinary disc initially hardens the binary, while the inner disc drains onto the primary (central) black hole. As long as the inner disc remains cool and thin at low $\dot{M}_{\rm ext}$ (rather than becoming hot and geometrically thick), the mass of the inner disc reaches an asymptotic mass typically $\sim 10^{-3} - 10^{-4} M_\odot$. Once the semimajor axis shrinks below a critical value, angular momentum losses from gravitational waves dominate over viscous transport in hardening the binary. The inner disc then no longer responds viscously to the inspiraling black holes. Instead, tidal interactions with the secondary rapidly drive the inner disc into the primary. Tidal and viscous dissipation in the inner disc lead to a late time brightening in luminosity, $L \propto t_{\rm minus}^{5/4}$, where $t_{\rm minus}$ is the time prior to the final merger. This late time brightening peaks ~ 1 day prior to the final merger at $\sim 0.1 L_{\rm Edd}$. This behavior is relatively robust because of self regulation in the coupled viscous-gravitational evolution of such binary systems. It constitutes a unique electromagnetic signature of a binary supermassive black hole merger and may allow the host galaxy to be identified if used in conjunction with the Laser Interferometric Space Antenna (LISA) localization.

Key words: black hole physics – accretion, accretion discs – binaries: general – gravitational waves – galaxies: active – galaxies: nuclei – quasars: general

1 INTRODUCTION

There is now strong evidence that supermassive black holes (SMBHs) inhabit the spheroids of most galaxies (Magorrian et al. 1998; Tremaine et al. 2002). Galaxy mergers, which are a natural consequence of hierarchical assembly of galaxies, should cause the SMBHs in each galaxy to form a binary in the newly assembled host galaxy (Begelman et al. 1980). These binary black holes (BBHs) are believed to coalesce due to an uncertain combination of dynamical friction, three body interactions, interaction with viscous circumbinary discs, and gravitational wave (GW) losses. Observations of the GW that these systems produce is one of the primary scientific objectives of the proposed Laser Interferometer Space Antenna (LISA). In addition to their usefulness as probes of general relativity in the strong field regime, GWs can also be used to measure the luminosity distance to high accuracy, i.e., $\delta D_{\rm L}/D_{\rm L}$ at the percent level in many cases (Hughes 2002; Holz & Hughes 2005).

The high accuracy that these "standard sirens" offer would allow these GW sources to constrain cosmological models if the host galaxy can be identified, so that a source redshift can be measured. By itself, LISA observations will provide sky localization errors that are typically $\sim$ few $\times 10^{-1}$ deg^2 (see for instance Holz & Hughes 2005; Kocsis et al. 2007, 2008; Lang & Hughes 2008; Arun et al. 2008), in which there may be $\sim 10^4$ galaxies.[1] Hence, much recent work has focused on finding an unambiguous electromagnetic counterpart to a BBH merger (Schutz 1986) to help identify its host galaxy. In addition, the known BH

⋆ E-mail: pchang@astro.berkeley.edu (PC); linda@astro.berkeley.edu (LES); kristen@astro.columbia.edu (KM); eliot@astro.berkeley.edu (EQ)

[1] The 3-D localization of LISA would give ~ 10 candidate galaxies per arcmin^{-2} (Holz & Hughes 2005; Kocsis et al. 2006).

masses and spins from GWs, an observed electromagnetic counterpart would also provide strong constraints on models of accretion discs and quasars/AGNs.

At present, most studies of these electromagnetic counterparts to BBH mergers have focused on the post-merger phase. At the time of merger, a fraction of the rest mass of the two BHs is radiated as GW and the merged BH receives a kick between $100 - 4000\,\mathrm{km\,s^{-1}}$ (Bekenstein 1973; Favata et al. 2004; Baker et al. 2006; Herrmann et al. 2007; González et al. 2007; Boyle et al. 2008). If a circumbinary gas disc surrounded the two BHs (pre-merger), the sudden decrease in BH mass and the kick provided by the BH may produce an observable electromagnetic signature (Bode & Phinney 2007; Lippai et al. 2008; Schnittman & Krolik 2008; Shields & Bonning 2008; O'Neill et al. 2008; Bode & Phinney 2009). On a longer timescale, the circumbinary disc would accrete into the newly merged BH, leading to AGN activity (Milosavljević & Phinney 2005) or perhaps an offset quasar (Madau & Quataert 2004).

There are potential difficulties associated with identifying these electromagnetic signatures of BBH mergers. The signatures associated with kicks are likely to be weak and difficult to distinguish from AGN variability, if they are a few percent of the background disc emission (Schnittman & Krolik 2008; Kocsis & Loeb 2008; O'Neill et al. 2008). Delayed AGN and offset AGN activity, while significantly more promising, might have a substantial delay (Milosavljević & Phinney 2005; Loeb 2007).

The subject of this work is to explore electromagnetic emission associated with the *pre-merger* phase. Various authors (Milosavljević & Phinney 2005; Armitage & Natarajan 2005; MacFadyen & Milosavljević 2008) have studied the physics of such viscously driven BBH mergers. These studies suggest that the interaction between the disc and the BBHs can induce a small eccentricity in the disc and the binary (Armitage & Natarajan 2005; MacFadyen & Milosavljević 2008; Cuadra et al. 2009). In addition, some of this gas may form accretion discs around the two BHs leading to binary AGN activity (Dotti et al. 2007).

In this paper, we build on the work of Armitage & Natarajan (2002) and show that although the inner disc drains when the binary is well separated, a small amount of remnant or fossil gas can remain around the primary BH, giving rise to a distinct electromagnetic signature. The amount of fossil gas is very small ($\sim 10^{-3} M_\odot$), but even this tiny amount of gas is sufficient to drive the luminosity of the binary to $\sim 0.1\,L_{\rm Edd}$ one day before merger.

The plan of this work is as follows. In §2, we summarize the basic scenario. We then present the relevant physics in §3. In §4, we argue that a small amount of fossil gas could exist in the inner disc between the primary and secondary BHs and that this fossil gas would be tidally driven into the primary on a very short timescale near the final merger, leading to a bright electromagnetic precursor. Finally in §5, we discuss some of the caveats of this model and directions for future work.

2 BASIC PICTURE

We illustrate the basic scenario schematically in Figure 1. A secondary BH with mass $M_{\rm sec}$ and a coplanar accretion disc orbits a more massive primary BH at a radius $r_{\rm sec}$. We expect the disc to be aligned to the orbital plane of the two BHs because of inclination damping. Ivanov et al. (1999) showed that in the case of a BH orbiting a more massive BH with an associated accretion disc, the inner accretion disc aligns with the orbit of the binary independent of the viscosity. As a result, the accretion disc is truncated into two parts: an inner accretion disc which surrounds the primary and a circumbinary disc which surrounds the binary. Flow between the inner disc and outer disc is prevented by the presence of the secondary BH at least in one dimension. The inner accretion disc has an inner radius, which is typically the innermost stable circular orbit (ISCO), and an outer radius where it is truncated due to tidal interactions with the secondary BH. Similarly, the outer disc is also truncated.

A similar model has previously been studied by Armitage & Natarajan (2002). However, we will include several improvements in our treatment. First we include more realistic physics for the evolution of the viscous disc, i.e., we use a self-consistent alpha disc instead of a fixed viscosity law. This significantly changes how the disc drains and we believe that it provides a more realistic estimate of the luminosity evolution of the disc prior to merger. Secondly, we focus on the luminosity of the late time electromagnetic precursor and its simple shape, which might aid its identification.

3 BASIC EQUATIONS

We now present the governing equations for our model. These are standard in the literature (Lin & Papaloizou 1979b,a, 1986; Hourigan & Ward 1984; Ward & Hourigan 1989; Rafikov 2002; Chang 2008; van de Ven & Chang 2008), but we state them here for completeness. We adopt the notation of Chang (2008) and van de Ven & Chang (2008). We also include the effect of angular momentum losses due to GWs, which become important at small binary separation.

The evolution of a viscous disc under the influence of an external torque is given by equations for continuity and angular momentum conservation.[2] The equation of continuity is (Frank et al. 2002)

$$\frac{\partial \Sigma}{\partial t} + \frac{1}{r}\frac{\partial (r \Sigma v_r)}{\partial r} = 0, \tag{1}$$

where r is the radial coordinate and v_r is the radial component of the velocity. The equation of angular momentum conservation is (Pringle 1981; Rafikov 2002):

$$\frac{\partial (\Sigma r^2 \Omega)}{\partial t} + \frac{1}{r}\frac{\partial (r v_r \Sigma r^2 \Omega)}{\partial r} = -\frac{1}{2\pi r}\left(\frac{\partial T_{\rm visc}}{\partial r} - \frac{\partial T_{\rm d}}{\partial r}\right), \tag{2}$$

where $\Omega = \sqrt{G M_{\rm BH}(r)/r^3}$ is the orbital frequency, $M_{\rm BH}$ is the mass of the primary BH, and

[2] For simplicity, we do not make a distinction between the center of mass of the binary and the location of the primary BH in our analysis, even though the secondary is not much less massive than the primary in some of our models.

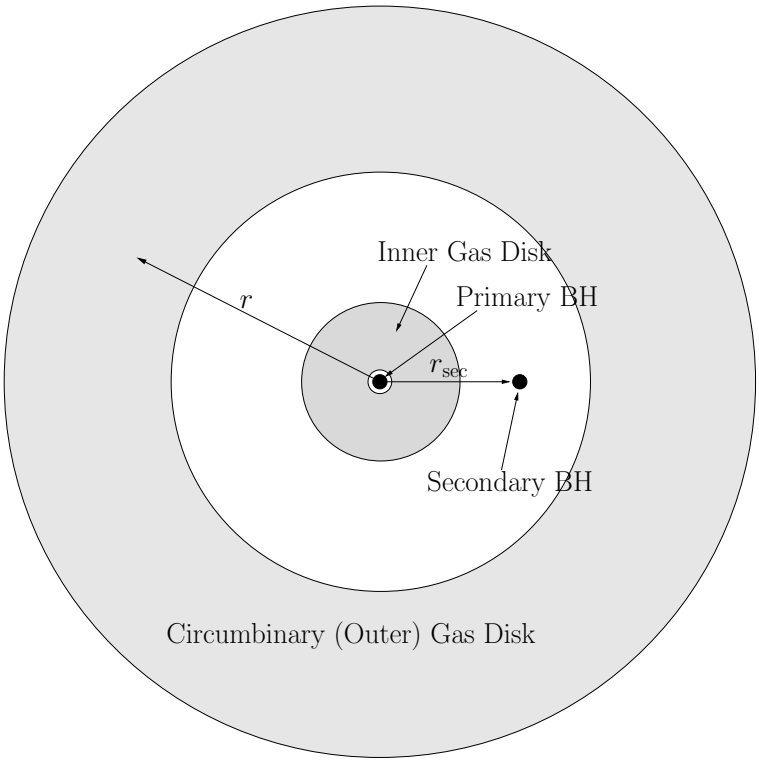

Figure 1. Schematic diagram of the model considered in this paper. An accretion disc and a secondary (coplanar) BH with semimajor axis $r_{\rm sec}$ surrounds a central BH. The secondary BH opens up a gap in the disc, dividing the disc into an inner disc and an outer disc. The inner disc steadily drains into the central BH, while the outer disc viscously spreads and tidally interacts with the secondary. The binary's semimajor axis decreases due to tidal interaction with the viscous disc until $r_{\rm sec} < r_{\rm GW}$, at which point GW emission becomes the primary mechanism by which angular momentum is lost. For $r_{\rm sec} \ll r_{\rm GW}$, the *inner* disc can no longer viscously respond on the merger timescale and is driven into the primary by tidal interactions with the secondary.

$$T_{\rm visc} = -2\pi r^3 \nu \Sigma \frac{\partial \Omega}{\partial r}, \tag{3}$$

is the viscous torque, where ν is the viscosity. We have adopted the standard α prescription for the viscosity (Shakura & Syunyaev 1973):

$$\nu = \frac{2\alpha P_{\rm g}}{3\Omega\rho}, \tag{4}$$

with proportionality to $P_{\rm g}$, the midplane gas pressure. We chose to rely on the so-called "β model", i.e., stress proportional to gas pressure as opposed to total pressure, to ensure viscous and thermal stability in our 1-d model. For most of our calculations, we use $\alpha = 0.1$.[3] A simple α-prescription applied to radiation pressure dominated discs is both viscously and thermally unstable (Lightman & Eardley 1974; Piran 1978). Recent work by Hirose et al. (2009) suggests that the thermal instability is avoided in radiation pressure dominated situations because stress fluctuations lead the associated pressure fluctuations. However, the viscous instability of radiation pressure dominated discs might remain. Adopting the "β model" for the viscous stress will only change the evolution at high $\dot{M}_{\rm ext}$ and small radius and does not affect our key results: once the binary is at small separation, the discs' evolution is dominated by GW losses and not by internal viscosity.

Using equation (1), we simplify (2) to be

$$\Sigma \frac{\partial (r^2\Omega)}{\partial t} + v_r \Sigma \frac{\partial (r^2\Omega)}{\partial r} = -\frac{1}{2\pi r}\left(\frac{\partial T_{\rm visc}}{\partial r} - \frac{\partial T_{\rm d}}{\partial r}\right). \tag{5}$$

Solving for v_r in equation (5) and plugging it into (1), we find

$$\frac{\partial \Sigma}{\partial t} = \frac{1}{2\pi r}\frac{\partial}{\partial r}\left(\frac{\partial (r^2\Omega)}{\partial r}\right)^{-1}\left[\frac{\partial}{\partial r}\left(T_{\rm visc} - T_{\rm d}\right)\right]. \tag{6}$$

The orbiting secondary BH exerts a torque density on the disc, $\partial T_{\rm d}/\partial r$, of the form (Goldreich & Tremaine 1980; Lin & Papaloizou 1979b; Ward 1997; Armitage & Natarajan 2002; Chang 2008):

$$\frac{\partial T_{\rm d}}{\partial r} \approx \frac{4}{9} f \,{\rm sgn}\left(r - r_{\rm sec}\right) \frac{G^2 M_{\rm sec}^2 \Sigma r}{\Omega^2 \left(r - r_{\rm sec}\right)^4}, \tag{7}$$

where f is a constant which is $\approx$ 0.1 following Armitage & Natarajan (2002).

Plugging equations (3) and (7) into (6), we find

$$\frac{\partial \Sigma}{\partial t} = \frac{1}{r}\frac{\partial}{\partial r}\left[3r^{1/2}\frac{\partial}{\partial r}\left(\nu\Sigma r^{1/2}\right) - \frac{4}{9\pi} f \,{\rm sgn}\left(r - r_{\rm sec}\right)\Omega r^2 q^2 \Sigma \left(\frac{r}{\left(r - r_{\rm sec}\right)}\right)^4\right], \tag{8}$$

[3] The exception is the suite of calculations presented in Table 1, where we have take $\alpha = 0.01$ and $\alpha = 0.1$

where $q = M_{\rm sec}/M_{\rm BH}$ is the mass ratio between the secondary and primary BHs.

The radial motion of the secondary BH, assuming a circular orbit, is governed by tidal torquing of the disc and the torque due to GWs:

$$\frac{1}{2}M_{\rm sec}\Omega_{\rm sec}r_{\rm sec}\frac{\partial r_{\rm sec}}{\partial t} = \frac{4}{9}fGM_{\rm BH}q^2\int \mathcal{S}\left(\frac{r}{r-r_{\rm sec}}\right)^4\Sigma dr - T_{\rm GW}. \quad (9)$$

where $\mathcal{S} = {\rm sgn}\,(r - r_{\rm sec})$ is the sign of the torque, and $T_{\rm GW}$ is the torque exerted by gravitational wave losses (Peters 1964),

$$T_{\rm GW} = \frac{\sqrt{8}}{5}M_{\rm BH}c^2\left(\frac{r_{\rm g}}{r_{\rm sec}}\right)^{7/2}\left(\frac{M_{\rm sec}}{M_{\rm BH}}\right)^2\sqrt{\frac{M_{\rm sec}+M_{\rm BH}}{M_{\rm BH}}}, \quad (10)$$

where $r_{\rm g} = 2GM_{\rm BH}/c^2$ is the Schwarzschild radius.

Finally we assume vertical energy balance at every radius between heating and radiative cooling, i.e. $F = D(r)$, where F is the local radiative flux and D is the local dissipation rate. In a one-zone model, the local radiative flux is

$$F = \frac{4}{3}\frac{\sigma T^4}{\kappa\Sigma}, \quad (11)$$

where T is the central temperature and κ is the opacity, which we assume to be constant (Thomson) for simplicity. More detailed models would include variations in opacity with radius in the disc. We assume that the disc emits as a blackbody. The heating is given by a combination of viscous dissipation and tidal dissipation. Viscous dissipation is given by the standard formula (Frank et al. 2002)

$$D_{\rm visc} = \frac{9}{8}\nu\Sigma\frac{GM_{\rm BH}}{r^3}, \quad (12)$$

where $D_{\rm visc}$ is the local viscous dissipation rate per unit area.

We now consider the energy dissipation from tidal torques. We assume that the torque on the disc raised by the satellite, $T_{\rm d}$, is mediated by the excitation of spiral density waves and locally damped. The timescale associated with this tidal torque is the angular momentum of the satellite, $L_{\rm sec} = M_{\rm sec}\Omega_{\rm sec}r_{\rm sec}^2$, divided by the torque or $t_{\rm tide} = L_{\rm sec}/T_{\rm d}$. The power associated with such a torque is then

$$\dot{E}_{\rm tide} = \frac{E_{\rm sec}}{t_{\rm tide}} = T_{\rm d}\Omega_{\rm sec}, \quad (13)$$

where $E_{\rm sec} = GM_{\rm BH}M_{\rm sec}/r_{\rm sec}$ is the orbital energy of the secondary. Because we assume local damping of spiral density waves, the corresponding binding energy liberated locally (assuming circular orbits) is in proportion to the spiral density waves which mediate this interaction. Hence the local tidal dissipation rate is given by

$$D_{\rm tide} = \frac{1}{2\pi r}\dot{E}_{\rm tide}\frac{|dT_{\rm d}/dr|}{\int dr|dT_{\rm d}/dr|}. \quad (14)$$

As we will show, these tidal interactions are especially important at late times when GW losses drive the secondary inward on a circular orbit. A tiny fraction ($M_{\rm d,in}/M_{\rm sec} \sim 10^{-10}$, where $M_{\rm d,in} \equiv 2\pi\int_0^{r_{\rm sec}}\Sigma r^2 dr$ is the mass of the inner disc) of the angular momentum losses is offset by a gain from the tidal interaction with the inner disc. The tidal-GW evolution allows this fraction of the prodigious gravitational luminosity $L_{\rm GW} < 10^{55}\,{\rm ergs\,s^{-1}}$,[4] to be released electromagnetically by heating the inner disc gas, which is enough to power the inner accretion disc close to its Eddington luminosity.

4 RESULTS

We solve equations (8) and (9) using standard explicit finite-difference methods (Press et al. 1992). We choose 200 grid points logarithmically spaced between $r = r_{\rm ISCO} = 3r_{\rm g}$ (i.e., the ISCO) and $10^5 r_{\rm g}$. We set a zero-torque boundary condition at the inner radius and impose an outer boundary condition such that there is a constant external feeding rate, $\dot{M}_{\rm ext}$. As a test, we initially solve these equations for no satellite and with inflow boundary conditions and find that we recover the steady state α-disc solution with an error of $\lesssim 1\%$.

The first two cases we consider are a $10^7 M_\odot$ BH with a $q = 0.1$ and a $q = 0.3$ secondary, respectively. We start the secondary at an initial radius of $r_{\rm s,0} = 10^4\,r_{\rm g}$ (≈ 0.01 pc). We begin with a low mass ($10^3 M_\odot$) disc which extends from the ISCO to $r_{\rm outer} = 10^5 r_{\rm g}$. We clear a region around the secondary's initial radius, $0.5r_{\rm s,0} < r < 2r_{\rm s,0}$, to model the initial clearing of a gap around the secondary BH. At the outer edge of the grid, we consider an outer $\dot{M}_{\rm ext}$ of either $\dot{M}_{\rm ext} = 0.1\,M_\odot\,{\rm yr}^{-1}$ or $0.01\,M_\odot\,{\rm yr}^{-1}$.

We choose a low initial disc mass ($10^3\,M_\odot$, which corresponds to a very low accretion rate in steady-state) so that our models can be integrated on a reasonable timescale. The reason is that the Courant condition, which is set by the viscous time of the disc near the ISCO, limits the timestep to very low values unless the disc has a very low mass. Fortunately, our results do not depend on this initial condition. The mass of the inner disc, $M_{\rm d,in}$, approaches an asymptotic value which is independent of its initial value. With larger initial disc masses, the inner disc would have initially drained on a faster time scale, but the final disc mass would remain the same.

We illustrate this point in Figure 2 where we show models with different disc masses of 10^2, 10^3, and $10^4 M_\odot$ for two different mass accretion rates: $\dot{M}_{\rm ext} = 10^{-1}\,M_\odot yr^{-1}$ (top set of curves) and $\dot{M}_{\rm ext} = 10^{-2}\,M_\odot yr^{-1}$ (bottom set of curves). Note that the mass of the inner disc approaches an asymptotic value that is independent of its initial value. The reason for this is that the inner disc drains until its viscous time is comparable to the merger time. At late times, however, when the evolution of the system is dominated by GWs, the inner disc can no longer viscously drain on the timescale of the merger. Hence, the inner disc mass is essentially frozen. The frozen mass of the inner disc at late times is given by the mass of the inner disc when the system transitions from viscosity-dominated evolution to GW-dominated evolution, which occurs typically at $r_{\rm GW} \sim 500 r_{\rm g}$ (Armitage & Natarajan 2002; Haiman et al. 2008, also see §4.2). In the remainder of this work, we use this fact and start with a low disc mass to save computational cost.

[4] The GW luminosity can maximally be $c^5/G \sim 3\times10^{59}\,{\rm ergs\,s^{-1}}$, but the GW luminosity when the disc is still present is closer to $\sim 10^{55}\,{\rm ergs\,s^{-1}}$

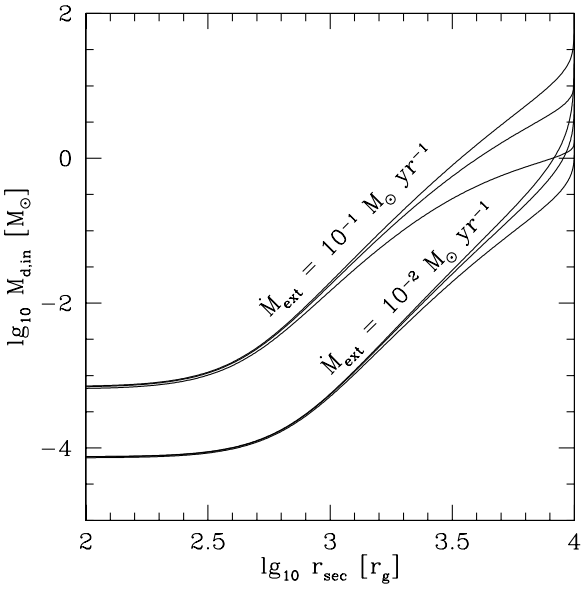

Figure 2. Evolution of the disc mass inside the secondary's orbital radius, $r_{\rm sec}$, for a $10^7\,M_\odot$ primary and $10^6\,M_\odot$ secondary and external mass accretion rates of $10^{-1}\,M_\odot yr^{-1}$ ($\dot{M}_{\rm ext} \approx \dot{M}_{\rm Edd}$; top set of curves), and $10^{-2}\,M_\odot yr^{-1}$ ($\dot{M}_{\rm ext} \approx 0.1\dot{M}_{\rm Edd}$; bottom set of curves). Three scenarios in each case, with initial disc masses of 10^4, 10^3, and $10^2\,M_\odot$, are represented by the curves from top to bottom. Note that the asymptotic disc mass is independent of the initial disc mass.

4.1 Viscous Evolution of the BBH and the Outer Disk

We first consider the case of a $10^7 M_\odot$ BH with a $10^6 M_\odot$ secondary and an outer mass inflow rate of $\dot{M}_{\rm ext} = 0.1 M_\odot\ {\rm yr}^{-1}$ (Figure 3) or $\dot{M}_{\rm ext} = 0.01 M_\odot\ {\rm yr}^{-1}$ (Figure 4). Figure 3 and 4 show four different cuts from our one-dimensional simulations to illustrate the different regimes through which the binary and the disc evolve with time. In each cut, we plot Σ (solid line matched to the left axis) and $t_{\rm visc}$ (dashed line matched to the right axis). We also show for each cut, the merger time of the BBH $t_{\rm merge}$ as a horizontal dotted line matched to the right axis. In (a), the satellite and binary have just been initialized and the outer disc has filled due to mass inflow from the outer boundary. In (b), the secondary's radius has decreased by an order of magnitude due to its tidal interaction with the viscously evolving outer disc. Meanwhile, the inner disc has drained substantially. In (c), the binary has shrunk by another order of magnitude in radius due to both tidal-viscous evolution and GW losses, with the latter becoming dominant at small radii. Note that the inner disc density profile has begun to invert, i.e., the surface density rises with radius as opposed to falling. This is due to the inability of the inner disc to viscously respond to the increasingly rapid infall of the secondary. By (d), a large surface density spike has built up near the outer edge of the inner disc. This forcing of the inner disc onto the primary BH causes it to brighten with a maximum luminosity, $L_{\rm peak}$, reached at a time, $t_{\rm peak}$, before the final merger.

A crucial aspect of the evolutionary sequence shown in Figure 3 and 4 is that, during the early phases (plots a and b; before GWs dominate), the viscous time, $t_{\rm visc} = r^2/\nu$ (dashed lines) near the outer edge of the inner disc adjusts to become comparable to the evolving merger time, $t_{\rm merge} = |r_{\rm s}/v_{\rm sec}|$ (shown as a horizontal dotted line in plots a and b). This implies that the evolutionary time for the inner disc is the same as the merger time of the binary. This adjustment occurs because a more massive disc would drain much more rapidly until it drains until the point where its viscous time equals the lifetime of the system. Similarly, a less massive disc would remain static until the external forcing from the secondary decreases the disc's outer radius and increases the local surface density to the point where the local viscous time matches the merger time. Hence the inner disc approaches an asymptotic state that just depends on the merger time of the binary. The binary merger time itself depends on the external feeding rate until gravitational waves take over. This self-regulated evolution explains lack of any difference of the inner disc mass on the initial disc mass shown in Figure 2. Note that once GWs dominate (plots c and d), $t_{\rm visc}$ does not adjust to $t_{\rm merge}$, the disc can no longer respond viscously to the rapidly infalling secondary and its dynamics becomes tidally dominated as shown vividly in panels (d) of Figures 3 and 4. The dissipation of tidal energy and the forcing of disc material to smaller and smaller radii is the primary means by which energy is produced in this late stage.

As Figure 3 and 4 show, the general evolutionary sequence of a BBH system can be summarized as follows. Initially the BBH starts out at large radii, where the tidal-viscous interaction with the outer gas disc shrinks the semi-major axis of the BBH. Meanwhile, the inner disc continually drains. Eventually, the BBH shrinks until $r < r_{\rm GW}$, where GWs become the principle mechanism by which angular momentum is lost. Shortly afterwards, the inner disc can no longer respond viscously to the inspiralling secondary and it reaches its asymptotic mass, $M_{\rm asym}$.[5] The inner disc is forced to smaller and smaller radii by the inspiraling secondary until it completely accretes onto the central BH. At this time, $t_{\rm peak}$ before the final merger, the inner disc has a peak luminosity, $L_{\rm peak}$. We have run a suite of models at different α, $\dot{M}_{\rm ext}$, $M_{\rm BH}$, and q to explore the parameter space of $M_{\rm d,in}$, $L_{\rm peak}$ and$t_{\rm peak}$. These results are summarized in Table 1 and discussed below.

4.2 The Electromagnetic Precursor of the BBH Merger

As Table 1 indicates, the peak luminosity of the electromagnetic precursor can be appreciable even though the asymptotic mass of the inner disc seems insignificant. The precursor's light curve is shown as a function of time prior to merger in Figure 5, where we plot the luminosity due to tidal and viscous dissipation as a function of the time before merger, $t_{\rm minus}$ (measured from when the BHs finally merge, which is not the same as the instantaneous merger time $r_{\rm sec}/|v_{\rm sec}|$) for the two cases of $M_{\rm BH} = 10^7 M_\odot$ (a) and $10^8 M_\odot$ (b). The results shown in Figure 5a are for the two mass inflow rates, $0.1 M_\odot\ {\rm yr}^{-1}$ (solid line) and $0.01 M_\odot\ {\rm yr}^{-1}$

[5] For consistency, we take the asymptotic disc mass, $M_{\rm asym}$, to be $M_{\rm d,in}$ at $r = 100 r_g$.

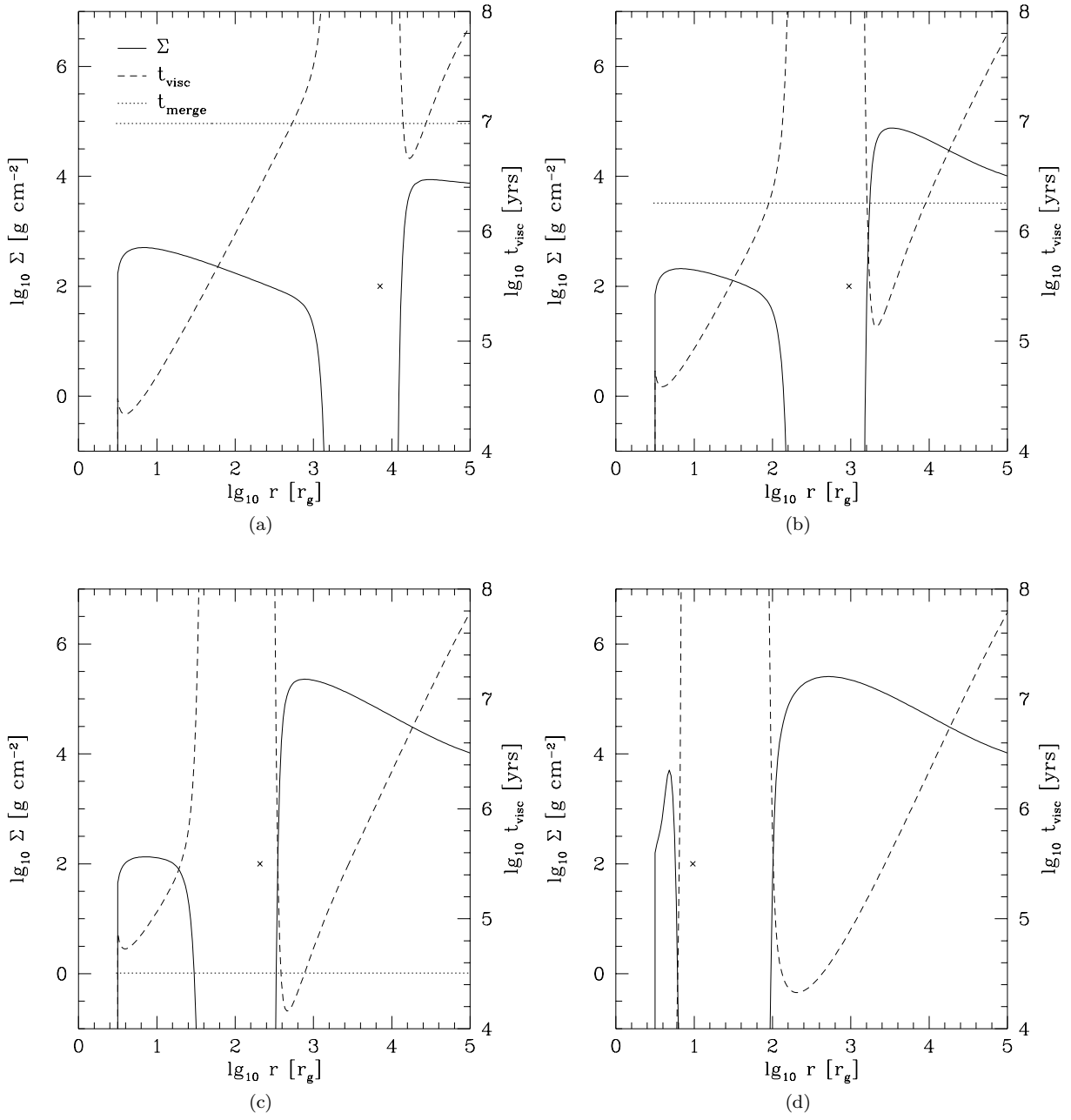

Figure 3. Snapshots of the disc properties for a $10^7 M_\odot$ primary BH with a $10^6 M_\odot$ secondary BH (whose position is marked with an "×"), for an external accretion rate of $10^{-1} M_\odot\,\mathrm{yr}^{-1}$. We plot the surface density Σ (solid lines), viscous time $t_{\rm visc}$ (dashed line, matched to right axis), and merger time of the secondary $t_{\rm merge}$ (dotted horizontal line, match to the right hand side). (a) shortly after initialization, when the outer disc has accumulated some mass due to accretion. (b) after the semimajor axis has decreased by an order of magnitude due to tidal-viscous interaction with the outer circumbinary disc. Note that the mass of the inner disc has declined significantly compared to (a) while the outer disc is approximately an alpha disc with a cutoff around the radial position of the secondary. (c) the semimajor axis has decreased by yet another order of magnitude, and the inner disc mass has reached it asymptotic value. Angular momentum losses are now dominated by GWs. (d) the secondary tidally forces the remaining mass in the inner disc to accrete rapidly into the central BH. It is this final forced feeding of the central BH which leads to the electromagnetic precursor (see Figure 5a,b).

(dashed line), and for $q = 0.1$ and $q = 0.3$ (top and bottom plots respectively). The electromagnetic precursor manifests itself as a sudden brightening to $\approx 0.1 - 1\, L_{\rm Edd}$ during the last few days before merger. There are a few notable characteristics of the light curve. The peak luminosity depends only on the mass of the inner disc. The time of the peak $t_{\rm peak}$ depends only on the masses of the two BHs. Finally, the light curve of the precursor has a very characteristic power-law shape.

The first two points are clear from examining Figure 5a,b. For instance for the $M_{\rm BH} = 10^7 M_\odot$ ($10^8 M_\odot$) case in Figure 5a(b), the characteristic shape and time of the peak

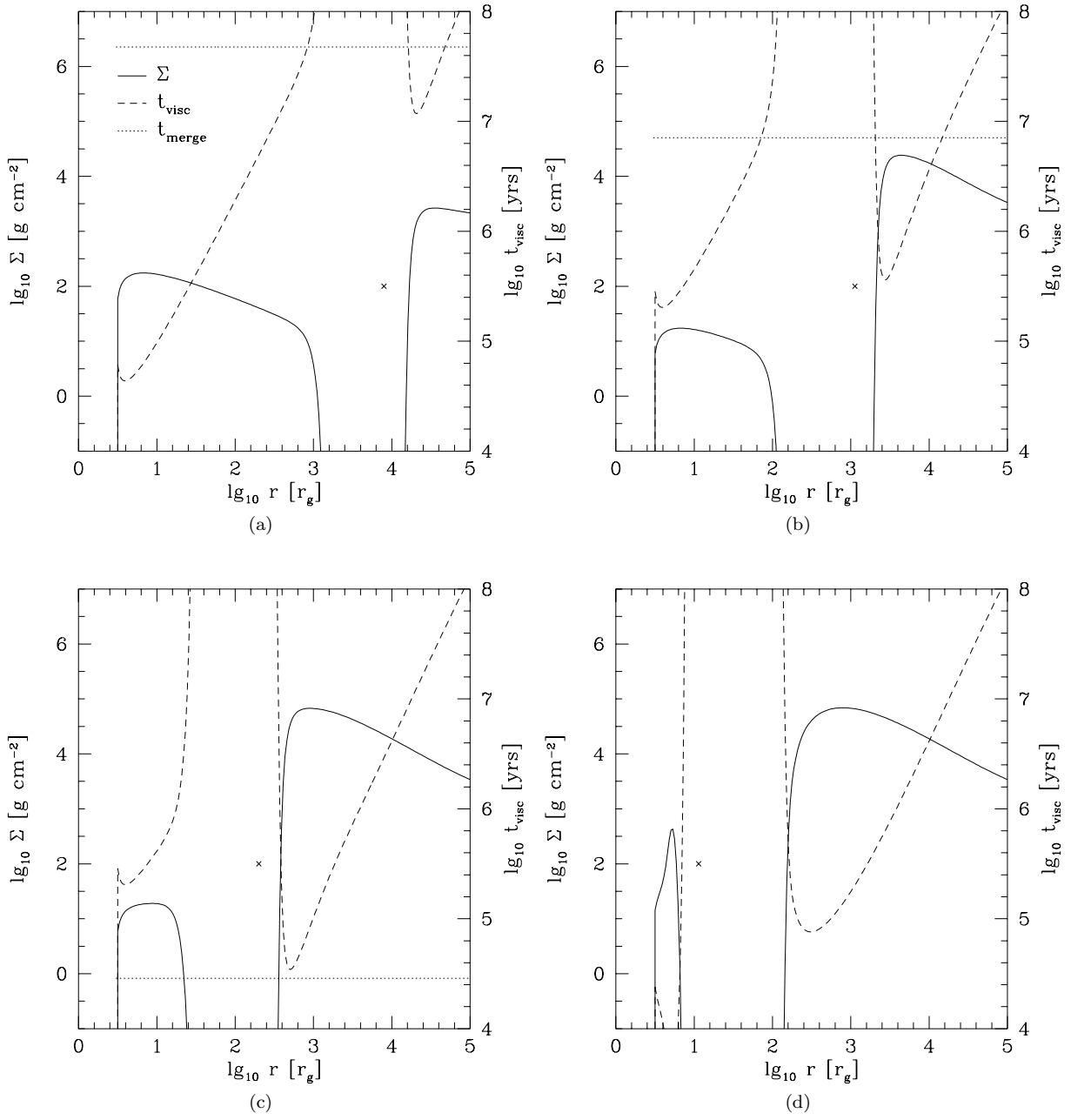

Figure 4. The same as Figure 3, but for an external accretion rate of $10^{-2} M_\odot\,\mathrm{yr}^{-1}$. The main notable difference is that the asymptotic mass of the inner disc is significantly smaller than for $\dot{M}_{\rm ext} = 10^{-1} M_\odot\,\mathrm{yr}^{-1}$ case of Figure 3.

of the light curve are the same for the two different $\dot{M}_{\rm ext}$s, but the normalization is different. The normalization of the light curve depends on the mass of the inner disc, which in turns depends on the outer mass accretion rate and α (see Table 1). On the other hand, the timescale of maximum luminosity only depends on the masses of the two BHs as one can see by comparing the cases $q = 0.1$ and $q = 0.3$ in Figure 5a,b.

The light curve follows a characteristic power law shape, which we now derive. Tidal interactions between the secondary BH and the accretion disc drive the outer edge of the disc to smaller radii and the dissipation of the induced density waves leads to heating of the disc. The amount of energy dissipated at any time is

$$L \approx \frac{G M_{\rm BH} M_{\rm d}}{r_{\rm sec}} t_{\rm merge}^{-1}, \tag{15}$$

where $M_{\rm d}$ is fixed as we are in a regime with the merging time much shorter than the viscous time. This mass is set primarily by the viscosity of the disc, i.e., α, and the external $\dot{M}_{\rm ext}$. It directly influences the luminosity of the inner disc in this GW driven phase of the merger. The merging timescale due to GWs is,

Table 1. Asymptotic inner disc mass and several quantities characterizing the EM precursor for a range of black hole masses, accretion rates, and α. We show $M_{\rm BH}$ [$M_\odot$], q, $\dot{M}_{\rm ext}$ [$M_\odot$ yr^{-1}], α, $M_{\rm asym}$ [$M_\odot$], $t_{\rm peak}$ [days], and $L_{\rm peak}$ [ergs s^{-1}].

$M_{\rm BH}$	q	$\dot{M}_{\rm ext}$	α	$M_{\rm asym}$	$t_{\rm peak}$	$L_{\rm peak}$
10^6				$\times 10^{-6}$		$\times 10^{43}$
	0.1	0.1	0.1	1.2	0.07	1.9
			0.01	12	0.07	3.6
		0.01	0.1	0.12	0.07	0.2
			0.01	1.2	0.07	0.38
	0.3	0.1	0.1	0.1	0.04	0.5
			0.01	1	0.04	0.3
		0.01	0.1	0.008	0.04	0.05
			0.01	0.1	0.04	0.027
10^7				$\times 10^{-4}$		$\times 10^{44}$
	0.1	0.1	0.1	6.6	0.7	2.0
			0.01	460	0.7	14
		0.01	0.1	0.73	0.7	0.23
			0.01	6.4	0.7	2.0
	0.3	0.1	0.1	0.62	0.4	0.19
			0.01	5.6	0.4	1.5
		0.01	0.1	0.062	0.4	0.019
			0.01	0.75	0.4	0.2
10^8				$\times 10^{-2}$		$\times 10^{45}$
	0.1	1	0.1	20	7	6.5
			0.01	90	7	28
		0.1	0.1	2.9	7	0.9
			0.01	18	7	5.7
	0.3	1	0.1	2.4	4	0.67
			0.01	15	4	4.2
		0.1	0.1	0.33	4	0.09
			0.01	3.3	4	0.9

$$t_{\rm merge} = \frac{5}{8}\frac{a}{c}\frac{M_{\rm BH}}{M_{\rm sec}}\left(\frac{a}{r_g}\right)^3. \quad (16)$$

Combining equations (15) and (16), we find

$$L \propto t_{\rm minus}^{-5/4}. \quad (17)$$

This power law shape is a good approximation to the light curve in the more detailed calculations in Figure 5a,b.

The associated effective temperature is $T_{\rm eff} \propto (L/r_{\rm d}(t)^2)^{1/4} \propto t_{\rm minus}^{-7/16}$. Figure 6 shows the corresponding multi-temperature blackbody spectra at $t_{\rm minus} = 1$ day and 10 days for $M_{\rm BH} = 10^7 M_\odot$ (left panel) and $10^8 M_\odot$ (right panel). These spectra are also shown for different mass ratios, $q = 0.1$ (thick lines) and $q = 0.3$ (thin lines), and for different outer accretion rates, $\dot{M}_{\rm ext} = \dot{M}_{\rm Edd}$ (solid lines) and $0.1\dot{M}_{\rm Edd}$ (dashed lines). As this plot demonstrates, the majority of the emission prior to merger will be in the extreme UV and soft X-ray. As a result, the electromagnetic precursor may be difficult to detect from the ground or in the presence of obscuration. We have presumed no reprocessing of the inner disc emission by the outer disc. If present, this may increase the luminosity of the source in more easily detectable wavelength, i.e., optical or near-IR, with possibly significant time delays. Large amplitude spiral density waves from the strong tidal forcing may contribute to non-thermal high energy emission. One notable aspect of these spectra is a gap in the emission between the low energy part, which is due to emission from the circumbinary disc, and the high energy part, which is due to emission from the tidally forced inner disc.

The mass in the inner disc can be dramatically affected if additional sources of mass inflow exist beyond the viscous condition considered here. For instance, if the gap between the inner disc and outer disc is not completely clear, then a small trickle of mass from the outer disc to the inner disc could change the asymptotic inner disc mass significantly. To quantify this point, at the transition radius between viscous and GW driven evolution, the mass drainage rate of the inner disc is

$$\dot{M} = \frac{M_{\rm in}}{t_{\rm merge}(r_{\rm GW})} \sim 10^{-10} - 10^{-9}\, M_\odot\, {\rm yr}^{-1}, \quad (18)$$

where $t_{\rm merge} = r_{\rm sec}/v_{\rm sec}$ is the instantaneous merger time. This very small mass inflow rate implies that any additional source of mass whose time averaged input rate over $t_{\rm merge} \sim 10^{6-7}$ yrs equals or exceeds equation (18) would greatly modify the inner disc evolution. The calculated asymptotic disc mass may thus be considered to be a conservative lower limit on the mass of the inner disc.

5 DISCUSSION AND CONCLUSIONS

We have calculated models of BBH evolution subject to torques from a circumbinary accretion disc and gravitational radiation losses. In general, the viscous time inside the orbit of the secondary BH is much less than the timescale for tidal-viscous interaction with the circumbinary disc to shrink the orbit of the binary. At first glance, this suggests that the inner disc should completely drain away. However, we have shown that the inner accretion disc maintains a small, but nontrivial residual mass (Fig.2), the value of which is set when GWs take over (at $r_{\rm GW} \sim 500 r_{\rm g}$) as the primary mechanism shrinking the orbit of the binary. This inner disc, which is then tidally forced into the primary by the secondary as it spirals inward, brightens significantly during the last day prior to merger. The bolometric luminosity rises as $t_{\rm minus}^{-5/4}$, peaking at one day with a peak luminosity of $\sim 0.1 L_{\rm Edd}$ for a representative $10^7\, M_\odot$ BH (see Table 1 for results for various αs, $M_{\rm BH}$, $\dot{M}_{\rm ext}$, and q)

Such an electromagnetic signature is very important for the identification of the host galaxies of BBH mergers, but our study is subject to several caveats. One such caveat is related to the persistence of a thin accretion disc at very low accretion rates. Studies of X-ray binaries suggest that below an accretion rate of $10^{-4} - 10^{-2}\dot{M}_{\rm Edd}$, accretion discs can transition from a thin radiatively efficient accretion disc to a thick radiatively-inefficient accretion flow (Gallo et al. 2003; Fender et al. 2004). If this were the case in our scenario prior to GW driven evolution, the inner disc would completely drain into the primary BH and hence the characteristic electromagnetic signature we have identified would be absent. We emphasize, however, that the inner disc asymptotically approaches a gas-supported, optically-thick thin disc solution, which in itself is stable at very low accretion rates. Thus it is not apriori obvious whether the transition to a geometrically thick disc must occur in all cases.

Our calculated mass for the inner disc represents a con-

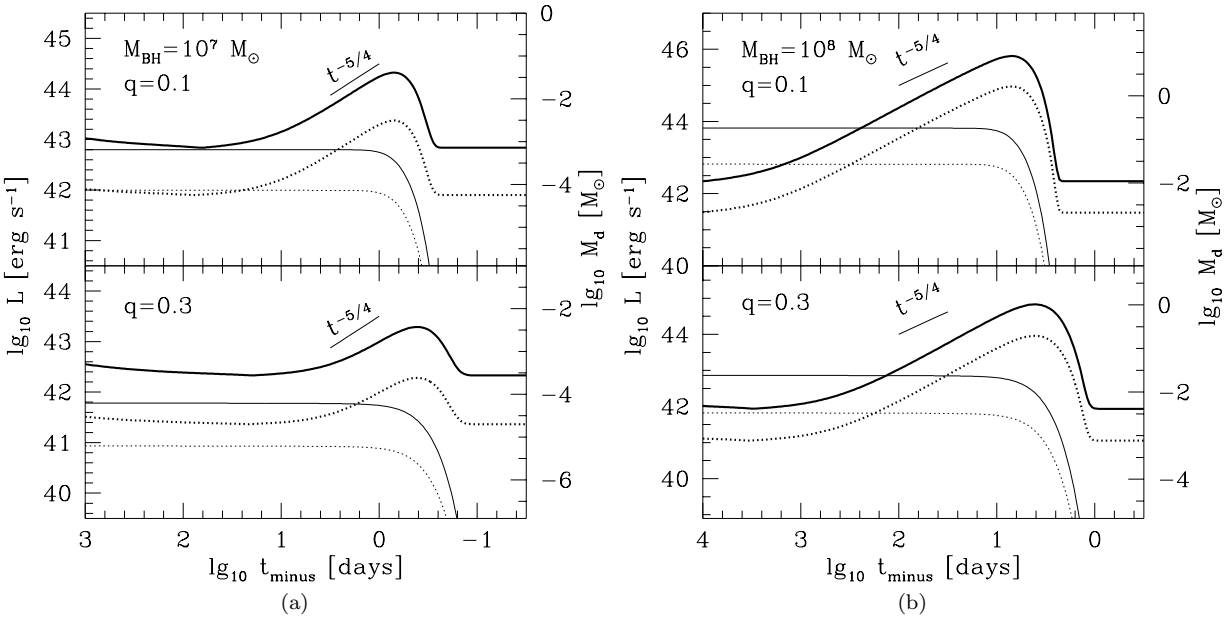

Figure 5. Bolometric luminosity (thick curves) and mass of the inner disc (thin curves) as a function of time before merger, $t_{\rm minus}$. (a) Evolution for a $10^7 M_\odot$ primary with a $10^6 M_\odot$ secondary (upper panel) and a $3\times10^6 M_\odot$ secondary (lower panel). We plot this evolution for $\dot{M}_{\rm ext} = 10^{-1}\,M_\odot\,{\rm yr}^{-1}$ (solid lines) and $\dot{M}_{\rm ext} = 10^{-2}\,M_\odot\,{\rm yr}^{-1}$ (dashed lines). (b) Similar evolution for a $10^8 M_\odot$ primary with a $10^7 M_\odot$ secondary (upper panel) and a $3\times10^7 M_\odot$ secondary (lower panel) and for $\dot{M}_{\rm ext} = 1\,M_\odot\,{\rm yr}^{-1}$ (solid lines) and $\dot{M}_{\rm ext} = 10^{-1}\,M_\odot\,{\rm yr}^{-1}$ (dashed lines). Note that the precursor approximately follows a $t_{\rm minus}^{-5/4}$ power law until the peak.

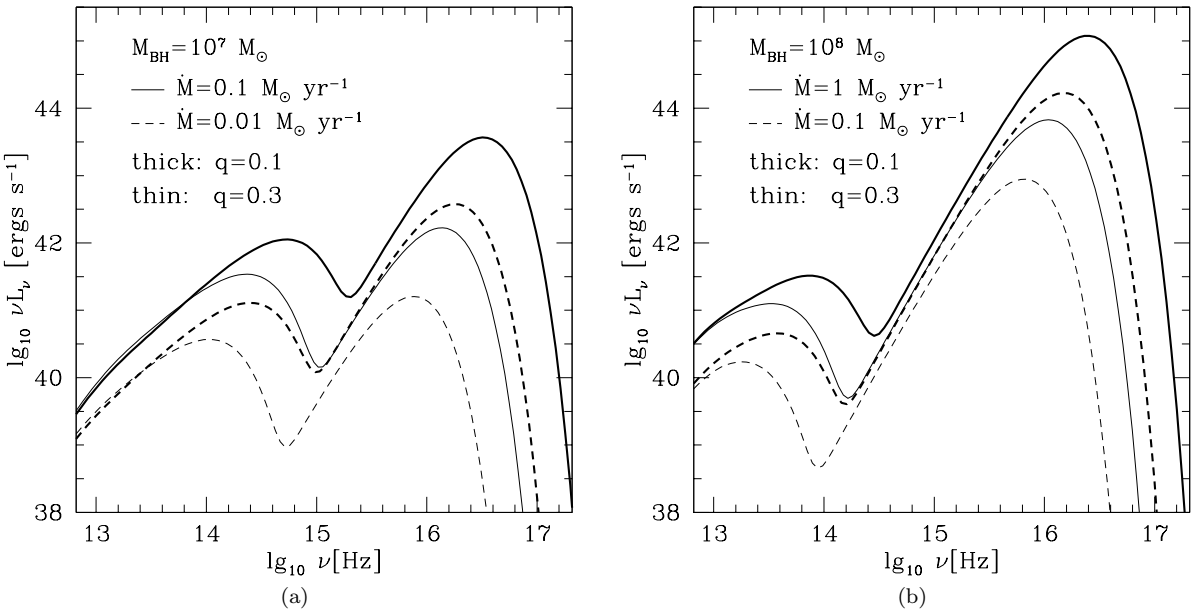

Figure 6. Multi-temperature blackbody spectra at $t_{\rm minus} = 1$ day for $M_{\rm BH} = 10^7 M_\odot$ (left) and at $t_{\rm minus} = 10$ days for $M_{\rm BH} = 10^8 M_\odot$ (right) in the evolutionary scenarios of Figure 5. Thick lines represent a mass ratio $q = 0.1$ and thin lines represent $q = 0.3$. Note the gap in the emission between the low energy component, which arises from the circumbinary disc, and the high energy component, which arises from the tidally forced inner disc.

servative lower limit. When the secondary transitions from a viscosity driven evolution to a gravitational wave driven evolution, the inner disc mass corresponds to a mass accretion rate of $\dot{M} \sim m_{\rm d}/t_{\rm merge} \sim 10^{-9}\,M_\odot\,{\rm yr}^{-1}$. For any time averaged mass source of cold gas present over $t_{\rm merge} \sim 10^6$–10^7 yrs that is greater than this, the mass of the inner disc would be larger than what we have calculated. For instance the mass loss from a few massive stars such as found in the Galactic center (Quataert 2004; Loeb 2004) or an old population of stars as in the nucleus of M31 (Chang et al. 2007), could easily enhance the mass of the inner disc. In addition, our one dimensional models presume that the gap between the inner and circumbinary disc is clean and that no mass flows between the two. While this may not be an unreasonable assumption given the comparable masses of the two BHs, two-dimensional simulations of gaps induced by protoplanets in a protoplanetary disc suggest that $\sim 10\%$ of $\dot{M}_{\rm ext}$ in the outer disc can flow across the gap onto the inner disc (Lubow & D'Angelo 2006; MacFadyen & Milosavljević 2008). Mass leakage across the gap in our case is likely to be much smaller than what it is in the protoplanetary case, but even a small amount of mass will make a substantial difference to the evolution of the inner disc.

We expect the perturbation to the GW signal from the tidal forcing of the inner disc to be minor in the sense that it would not be detectable with LISA. In the final year of inspiral, the inner disc has reached its asymptotic mass of $\sim 10^{-2} - 10^{-4} M_\odot$ (see Figure 5a,b). In this stage, the inner disc modifies the torque from GWs by a factor of $M_{\rm d}/M_{\rm sec} \sim 10^{-10}$. Such a tiny mass correction is well below the best achievable precision on mass measurements for the secondary with LISA (e.g., Hughes 2002; Lang & Hughes 2008).

The tidal forcing of an accretion disc by a spiraling binary is a somewhat unusual situation in astrophysics and the possibility that it occurs in the mergers of BBHs motivates further exploration of the physics of this scenario. One interesting possibility is that the precursor re brightening event that we have identified could be time-variable due to perturbations from the orbiting secondary. This is analogous to the case of superhumps, where perturbations from a low mass secondary drives the disc in a cataclysmic variable system to be mildly eccentric (Lubow 1991). A similar eccentricity growth has been suggested for the outer disc of BBHs by MacFadyen & Milosavljević (2008) and Cuadra et al. (2009). Time variability on the binary's period (or some multiple) would allow for an unambiguous association of the electromagnetic signal with the GW signal measured from future gravitational wave detectors such as LISA. The emergence of a time variable signal from the tidally forced accretion of this fossil gas is worthy of further investigation.

ACKNOWLEDGMENTS

We thank L. Bildsten for useful discussions. P.C. thanks Kavli Institute for Theoretical Physics for their hospitality during the completion of this work. This research was supported in part by the National Science Foundation under Grant No. PHY05-51164 and by NASA under Grant No. NNX08AH35G. P.C. is supported in part by the Miller Institute for Basic Research. K.M. thanks the Aspen Center for Physics for hospitality during the completion of this work. E.Q. is supported in part by NASA grant NNG06GI68G and the David and Lucile Packard Foundation.

REFERENCES

Armitage P. J., Natarajan P., 2002, ApJL, 567, L9
Armitage P. J., Natarajan P., 2005, ApJ, 634, 921
Arun K. G., Babak S., Berti E., Cornish N., Cutler C., Gair J., Hughes S. A., Iyer B. R., Lang R. N., Mandel I., Porter E. K., Sathyaprakash B. S., Sinha S., Sintes A. M., Trias M., Van Den Broeck C., Volonteri M., 2008, ArXiv e-prints
Baker J. G., Centrella J., Choi D.-I., Koppitz M., van Meter J. R., Miller M. C., 2006, ApJL, 653, L93
Begelman M. C., Blandford R. D., Rees M. J., 1980, Nature, 287, 307
Bekenstein J. D., 1973, ApJ, 183, 657
Bode J. N., Phinney E., 2009, in American Astronomical Society Meeting Abstracts Vol. 213 of American Astronomical Society Meeting Abstracts, Observability of Circumbinary Disks Following Massive Black Hole Mergers
Bode N., Phinney S., 2007, APS Meeting Abstracts
Boyle L., Kesden M., Nissanke S., 2008, Physical Review Letters, 100, 151101
Chang P., 2008, ApJ, 684, 236
Chang P., Murray-Clay R., Chiang E., Quataert E., 2007, ApJ, 668, 236
Cuadra J., Armitage P. J., Alexander R. D., Begelman M. C., 2009, MNRAS, 393, 1423
Dotti M., Colpi M., Haardt F., Mayer L., 2007, MNRAS, 379, 956
Favata M., Hughes S. A., Holz D. E., 2004, ApJL, 607, L5
Fender R. P., Belloni T. M., Gallo E., 2004, MNRAS, 355, 1105
Frank J., King A., Raine D. J., 2002, Accretion Power in Astrophysics: Third Edition. Accretion Power in Astrophysics, by Juhan Frank and Andrew King and Derek Raine, pp. 398. ISBN 0521620538. Cambridge, UK: Cambridge University Press, February 2002.
Gallo E., Fender R. P., Pooley G. G., 2003, MNRAS, 344, 60
Goldreich P., Tremaine S., 1980, ApJ, 241, 425
González J. A., Hannam M., Sperhake U., Brügmann B., Husa S., 2007, Physical Review Letters, 98, 231101
Haiman Z., Kocsis B., Menou K., 2008, ArXiv e-prints
Herrmann F., Hinder I., Shoemaker D., Laguna P., Matzner R. A., 2007, ApJ, 661, 430
Hirose S., Krolik J. H., Blaes O., 2009, ApJ, 691, 16
Holz D. E., Hughes S. A., 2005, ApJ, 629, 15
Hourigan K., Ward W. R., 1984, Icarus, 60, 29
Hughes S. A., 2002, Phys. Rev. D, 66, 102001
Ivanov P. B., Papaloizou J. C. B., Polnarev A. G., 1999, MNRAS, 307, 79
Kocsis B., Frei Z., Haiman Z., Menou K., 2006, ApJ, 637, 27
Kocsis B., Haiman Z., Menou K., 2008, ApJ, 684, 870
Kocsis B., Haiman Z., Menou K., Frei Z., 2007, Phys. Rev. D, 76, 022003

Kocsis B., Loeb A., 2008, Physical Review Letters, 101, 041101
Lang R. N., Hughes S. A., 2008, ApJ, 677, 1184
Lightman A. P., Eardley D. M., 1974, ApJL, 187, L1+
Lin D. N. C., Papaloizou J., 1979a, MNRAS, 188, 191
Lin D. N. C., Papaloizou J., 1979b, MNRAS, 186, 799
Lin D. N. C., Papaloizou J., 1986, ApJ, 307, 395
Lippai Z., Frei Z., Haiman Z., 2008, ApJL, 676, L5
Loeb A., 2004, MNRAS, 350, 725
Loeb A., 2007, Physical Review Letters, 99, 041103
Lubow S. H., 1991, ApJ, 381, 259
Lubow S. H., D'Angelo G., 2006, ApJ, 641, 526
MacFadyen A. I., Milosavljević M., 2008, ApJ, 672, 83
Madau P., Quataert E., 2004, ApJL, 606, L17
Magorrian J., Tremaine S., Richstone D., Bender R., Bower G., Dressler A., Faber S. M., Gebhardt K., Green R., Grillmair C., Kormendy J., Lauer T., 1998, AJ, 115, 2285
Milosavljević M., Phinney E. S., 2005, ApJL, 622, L93
O'Neill S. M., Miller M. C., Bogdanovic T., Reynolds C. S., Schnittman J., 2008, ArXiv e-prints
Peters P. C., 1964, Physical Review, 136, 1224
Piran T., 1978, ApJ, 221, 652
Press W. H., Teukolsky S. A., Vettering W. T., Flannery B. P., 1992, Numerical Recipes. Cambridge Univ. Press, Cambridge
Pringle J. E., 1981, ARA&A, 19, 137
Quataert E., 2004, ApJ, 613, 322
Rafikov R. R., 2002, ApJ, 572, 566
Schnittman J. D., Krolik J. H., 2008, ApJ, 684, 835
Schutz B. F., 1986, Nature, 323, 310
Shakura N. I., Syunyaev R. A., 1973, A&A, 24, 337
Shields G. A., Bonning E. W., 2008, ApJ, 682, 758
Tremaine S., Gebhardt K., Bender R., Bower G., Dressler A., Faber S. M., Filippenko A. V., Green R., Grillmair C., Ho L. C., Kormendy J., Lauer T. R., Magorrian J., Pinkney J., Richstone D., 2002, ApJ, 574, 740
van de Ven G., Chang P., 2008, ApJ in press, ArXiv e-prints, 0807.2437
Ward W. R., 1997, Icarus, 126, 261
Ward W. R., Hourigan K., 1989, ApJ, 347, 490